

DYNAMIC FRACTURE TESTING USING CHARPY INSTRUMENTED PENDULUM

Z. Radakovic ¹, Gy. B. Lenkey ², V. Grabulov ³, A. Sedmak ¹, D. Radakovic ⁴

¹ Department of Mechanical Engineering, University of Belgrade,
27. marta 80, 11220 Belgrade, Yugoslavia

² Bay Zoltán Institute for Logistics and Production Systems, Department for Structural Integrity
Iglói u. 2, 3519 Miskolc, Hungary

³ Military Technical Institute, Niska bb, 11132 Belgrade, Yugoslavia

⁴ Methode Electronics Malta Ltd., Mriehel Industrial Estate, Mriehel QMR09, MALTA

ABSTRACT

Charpy impact testing of a high strength low-alloyed (HSLA) steel has been performed by simultaneously recording two independent signals. The magnetic emission (ME) and potential drop (PD) techniques were used to determine critical crack initiation properties on standard V-notched and pre-cracked three-point bending specimens at room temperature. Both signals (ME and PD) were recorded and compared, with the purpose of more precise identification of critical fracture mechanics parameters determining the onset of ductile crack growth. Standard Charpy specimens made of HSLA steel, oriented perpendicular to rolling direction were tested by a modified instrumentation of the Charpy machine, which included the original magnetic emission, and the potential drop techniques. The strain gauges and emission probes, located on the hammer tup, measured the force, thus both the magnetic and electric potential drop signals were monitored and recorded as a function of time. The obtained results indicate good agreement between ME and PD techniques on evaluation of ductile crack growth initiation point.

KEYWORDS

Dynamic fracture, crack initiation, impact tests, fracture toughness, magnetic emission, potential drop

INTRODUCTION

The instrumentation of the Charpy testing machine by two independent techniques has been successful for dynamic fracture testing of the high strength micro-alloyed steel. The magnetic emission (ME) technique has been used for dynamic fracture testing by depicting the stable and unstable crack initiation [1], and has been applied for impact testing of certain types of steels, including railroad and reactor pressure vessel steels [2,3,4], as well as the HSLA steel [5]. In the case of ductile, or ductile/cleavage fracture, at temperatures well above nil-ductile, or at lower impact energies, it is sometimes difficult to distinguish the crack initiation event directly from the ME signal, and even the integrated ME signal sometimes has a slower rate of change, resulting in a plateau-like region without clear discontinuity. Alternatively, the potential drop method (PD) was also applied for the same purpose by recording the change in electrical resistance by drop in electric potential (PD) in the vicinity of the crack tip [6,7]. Results have also been obtained by applying this

technique on a single specimen with a particular method for evaluating the R-curve for HSLA steels [8,9]. Stable crack initiation in this case is similarly depicted from the local minimum (or maximum) of the potential drop value and, as in the case of ME technique, may not give clear local extreme values when conditions of fracture change from brittle to ductile [5]. As expected, results obtained from testing specimens at several loading rate (or impact velocity) have shown that the change of slope in the PD-t diagram can be used to evaluate critical crack behaviour, and if compared to similar changes of slope in the MF-t diagram, or vice versa, can eliminate doubts and provide a better understanding of both diagrams and measurement techniques. Some preliminary investigations have already been discussed [10].

Therefore, the two techniques were implemented in a Charpy instrumentation that gave independent and simultaneous records of ME and PD signals and the results were not only compared to check their validity, but to portrait the essence of superimposing all the benefits that characterize a certain testing technique.

MATERIAL AND EXPERIMENT

Micro-alloyed steels have a wide range of use in gas and oil pipelines, storage tanks, pressure vessels, vehicles, cranes, and metal structures in general. The tested steel is micro-alloyed with Nb and Ti and is obtained by controlled rolling and accelerated cooling, providing a ferrite-pearlite microstructure. With a yield stress of 411 MPa, the material is very ductile, even at lower temperatures, with a nil-ductility temperature below -80°C . The chemical composition (in wt. %) is shown in Table 1.

TABLE 1
CHEMICAL COMPOSITION IN WEIGHT PERCENT

C	Si	Mn	P	S	Al	Cu	Cr	Ni	Mo	Nb	Ti
0.08	0.20	1.12	0.027	0.011	0.033	0.065	0.027	0.019	0.010	0.026	0.017

The ferritic-pearlitic steel exhibits upper shelf values for ductile type of fracture at room temperature. This type of fracture is evident from load-time or load-displacement data. All the tests were performed at room temperature, owing to certain limitations of the PD technique [9]. The specimens were tested using initial energy levels in the range of $E_0=26\div 70$ J, enabling different impact loading rates between $v_0=1.69\div 2.75$ m/s. The fracture toughness of the material is affected by the impact velocity, and in ductile materials, the fracture mechanism is controlled by the strain field. This property may increase or decrease, depending on the loading rate [9,11]. The introduced fatigue cracks, that also influence the fracture toughness, are within the range: $a/W=0.47\div 0.57$.

The standard V-notched Charpy specimens were cut from a 12 mm plate perpendicular to rolling direction. All specimens were pre-cracked by high frequency fatigue. Since potential drop measurement requires additional specimen preparation, specimens were prepared in the manner explained by Grabulov [9]. Fig. 1 shows the prepared specimen on the anvil of the Charpy machine with the required instrumentation. Very thin wire connections for potential signal output were resistance-spot-welded to the specimen at asymmetric positions in respect to the notch (locations A, Fig. 1), being the optimal position. Apparently, the spot welding technique was performed by selecting inadequate welding parameters, resulting in loose contacts. The output wires were produced of steel, Ni, or Ni-Cr alloy, so some connections had to be re-connected in an unfavourable manner, by soldering. The heavier input Cu-wires originating from the DC power source were connected to the specimens by bolts (position III), securing a firm contact. The nominal input DC electric current of 30 A was required in order to produce output potential drop values ranging from several to at least 10 mV. This input DC value was selected as a minimum, and for some specimens it was increased up to 40 A, and even 50 A in order to amplify the weak output PD signal. Another limiting effect appeared from these wire connections as well. Being rather large and massive, they influenced the inertia characteristic of the specimens, and produced a problem that has yet to be solved – interrupted specimen fracture at higher loading rates, because of mutual contact and/or collision of these wire-connections with the inclined anvil

wall surface when gradual specimen bending commences during impact. However, this appeared much later after crack initiation, and did not produce any unwanted effects within the investigated time window. The magnetic emission probe (ME) on the hammer tup recorded changes in the external magnetic field in the vicinity of the propagating crack, Fig. 1. The calibrated strain gauge on the tup acted as a load transducer. Sophisticated data acquisition equipment consisted of a DC signal amplifier and voltage supply, both tied to a TEKTRONIX TDS 420A digital oscilloscope. The transient recorder, with an interior circuit amplifier, was tied to the remaining channel on the oscilloscope. The load was measured by strain gauges and emission probes on the hammer, and both magnetic and electric potential drop signals were monitored and recorded in real sampling time intervals of 2, 4, 10 and 40 microseconds. All acquired data was then handled by PC spreadsheet procedures, including the evaluation of absorbed energy (U) and the critical dynamic J-integral.

In order to check whether the ME instrumentation influenced PD measurements, and vice versa, the first two specimens were tested by applying techniques separately. The other specimens were tested simultaneously, with no record of signal interference, or other disturbing effects on the recorded signals. The high noise ratio in the PD signal is probably due to the poor grounding or it may have originated from nearby installations, but did not influence the character of the signal. This was minimized to a certain degree by toggling the input coupling impedance on the PD channel from 1 MΩ to 50 Ω, and also by analysing the diagrams and several multi-point linear trendlines in spreadsheet analyses. On the other hand, the ME signal retained good quality, having much less noise.

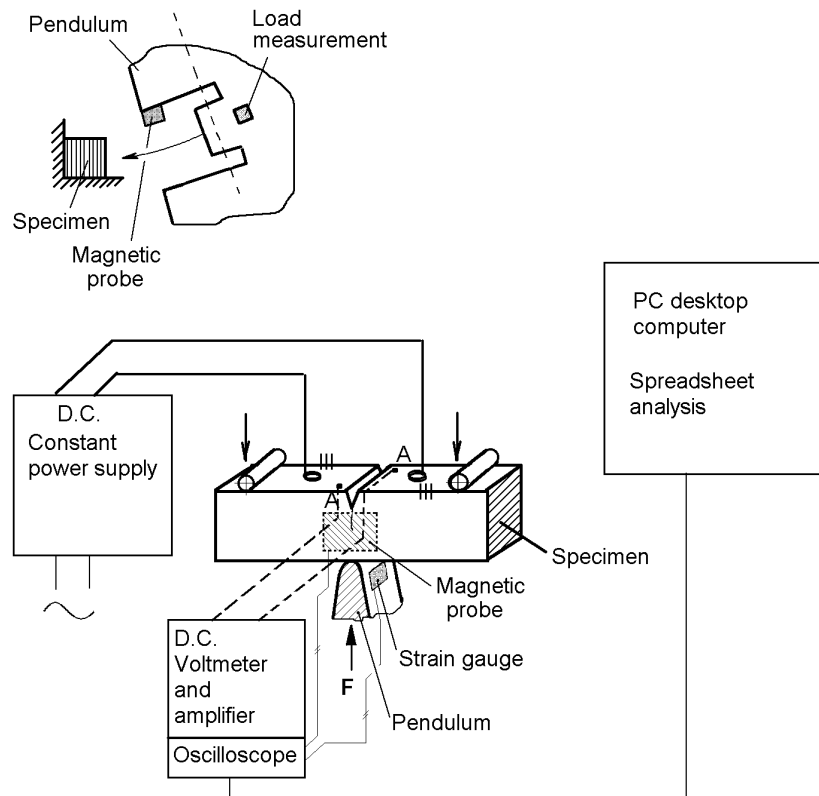


Figure 1. The Charpy pendulum instrumentation

RESULTS AND DISCUSSION

In the case of complete ductile fracture, the fracture toughness is calculated from the J-integral values under dynamic conditions (J_c^d), and is denoted by K_{Id} , whereas in the case of mixed fracture, especially when the ratio of elastic strain energy is not negligible, calculations should then include brittle and ductile fracture, separately ($J_{el} + J_{pl}$). In these tests fracture was generally ductile ($J_{el} < 0.03 J_{pl}$). The obtained results shown in Table 2 and in Figs. 2 and 3 clearly indicate a satisfying agreement between ME and PD tests on the evaluation of ductile crack growth initiation for this type of HSLA steel.

The J-integral at the initiation of the stable crack growth under dynamic conditions (J_I^d) is determined from Eq. (1), given below

$$J_{Ii}^d = \frac{2U_i}{B_n(W-a)}, \quad \text{where } i = \begin{cases} m, & \text{with results from ME tests} \\ pd, & \text{with results from PD tests} \end{cases} \quad (1)$$

The released energy – U_m or U_{pd} , is integrated from the load–displacement curve $F(t)$ - $f(t)$ by using

$$U_i = \int_0^{f_c} F(f)df \quad (2)$$

where the displacement at stable crack growth initiation $f_c(t)$ is determined at a time-to-stable crack initiation interval (t_i) or by time-to-fracture (t_F), whose determination is sometimes a difficult task, especially in the case of complete ductile fracture, when recorded diagrams, ME(t) and PD(t), do not always show a clear discontinuity. In these circumstances, it is necessary to analyze and compare all other diagrams as well: F(t), integrated-ME(t) (or MF(t)), or several multi-point linear or polynomial PD(t)-trendlines. This is a crucial moment when simultaneous implementation of two independent techniques is a benefit. In cases when diagrams acquired from a single technique cannot be distinguished, as an alternative, the other testing technique gave complementary diagrams.

As an example of good agreement, specimen C11 results are shown on diagrams F(t)-MF(t) and F(t)-PD(t) in Figs. 2 and 3. Table 2 contains relevant data for some HSLA steel specimens, tested at 20°C. Columns include: pre-crack length– a_o ; impact load rate– v_o ; maximum impact load– F_{max} ; time to stable crack initiation – t_i (or time-to-fracture– t_F), and calculated relative time difference between ME and PD tests– $\Delta(t_i)$; released energy– U ; calculated dynamic J-integral from ME and PD tests– J_{cm}^d , J_{cpd}^d , and the relative absolute difference between dynamic J-integrals calculated from ME and PD tests– $|\Delta(J_c^d)|$.

Table 2 - Measured and calculated results from ME and PD impact tests

Specimen id.	a_o	b_m	v_o	F_{max}	$t_i, \mu s$		$\Delta(t_i)$	U, J		$J_c^d, kJ m^{-2}$		$ \Delta(J_c^d) $
	mm	mm	$m s^{-1}$	kN	ME	PD	%	ME	PD	ME	PD	%
A4 Ni *	5.60	7.03	1.69	4.59	920	940	-2.2	3.68	3.81	167.3	173.2	7.7
B1	5.37	6.77	1.81	5.62	1160	1190	-2.6	4.59	4.84	198.2	208.9	14.1
B3 Ni	5.70	7.65	1.82	4.96	540	500	7.4	3.56	3.27	165.4	152.0	5.5
B14	5.30	6.83	1.82	5.84	610	530	13.1	4.78	4.08	203.2	173.6	4.5
A7 NiCr	5.57	7.75	1.82	5.16	800	790	1.3	4.35	4.28	196.4	192.9	3.5
C10 Ni	4.70	6.62	2.09	6.17	1160	1040	10.3	6.77	5.45	255.4	205.7	0.0
C15	5.12	7.93	2.22	5.67	640	640	0.0	4.51	4.51	184.8	184.8	0.0
C11	4.83	7.72	2.33	6.54	800	770	3.8	4.88	4.51	188.9	174.6	0.0
B16	5.27	9.40	2.55	5.60	460	452	1.7	4.71	4.61	198.9	194.7	2.1
B17	5.37	9.40	2.55	5.59	530	480	9.4	5.03	4.42	217.1	190.8	10.9
A5 Ni	5.47	9.35	2.56	5.37	528	440	16.7	4.95	3.93	218.4	173.3	2.0
A6 NiCr	5.38	9.37	2.56	5.14	460	458	0.4	4.39	4.36	190.1	189.1	0.5
B20	5.30	9.17	2.56	5.43	640	684	-6.9	4.85	5.37	206.5	228.7	4.1
B19	5.37	9.27	2.75	5.66	490	490	0.0	4.48	4.48	193.4	193.4	5.5
C2	5.22	9.35	2.75	5.77	560	550	1.8	5.17	5.03	216.0	210.2	2.7

*) Some specimen identification also notes the material type of the PD output wire connections

Some diagrams, F(t)-ME(t) or F(t)-PD(t), may not provide exact information about stable crack initiation time, and so they were averaged, Figs. 2 and 3. Usually, the change of slope in the F(t)-MF(t) diagram, and the local extreme point in the F(t)-PD(t) diagram (normal or average) is used instead (Fig. 3). This is also in agreement with the physical meaning of ME and MF quantities [2,3]. In the case of PD signal, stable crack initiation time is evaluated directly [9].

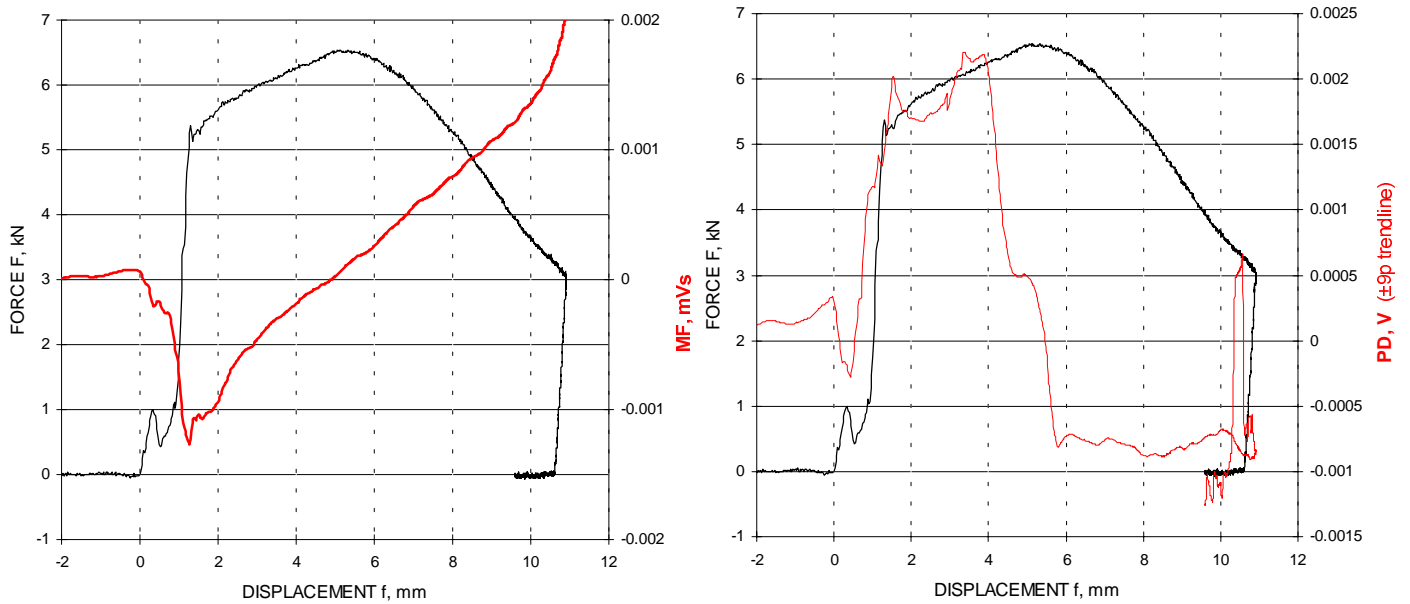


Figure 2. F(t)-f(t) diagrams with MF and PD signals for specimen C11 ($E_o=50$ J; $a_o/W=0.48$; PD input 50 A; insulated)

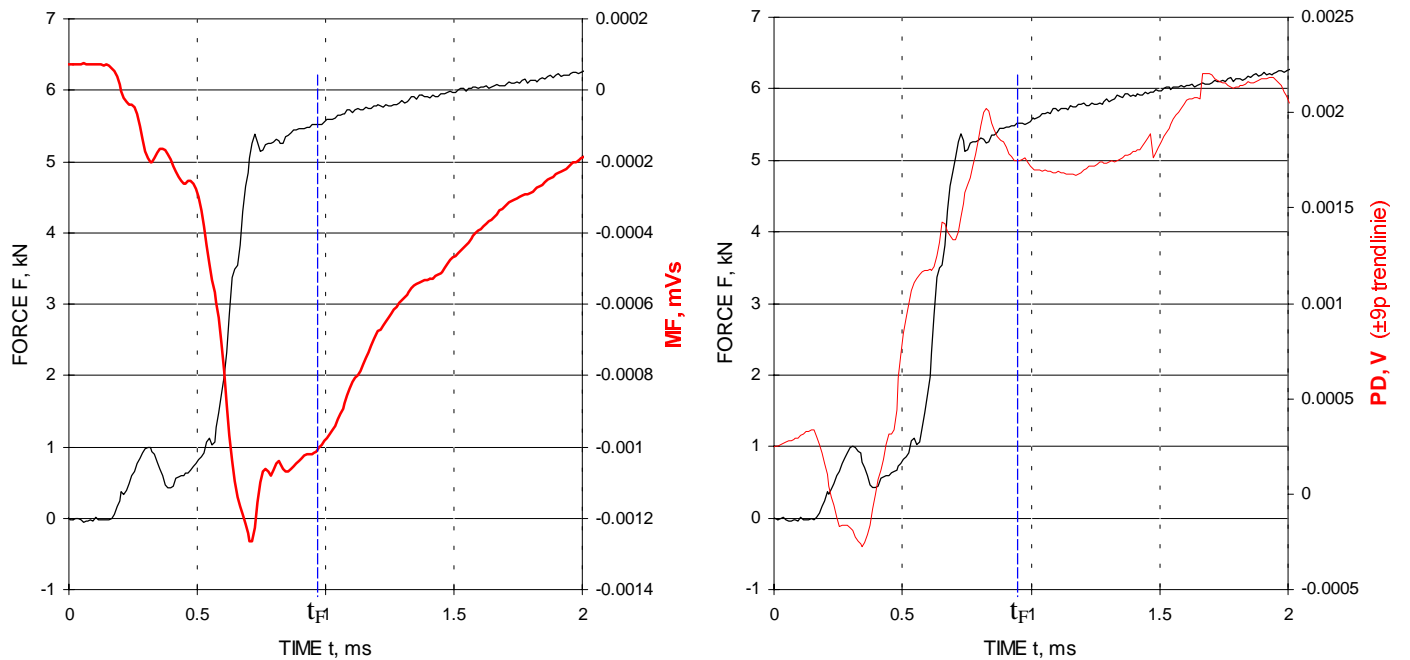


Figure 3. F(t) diagrams with MF and PD signals for specimen C11, indicating time-to-fracture (t_F)

The relative difference between critical values of dynamic J-integral is very low, with an absolute average $|\Delta(J_c^d)|_{aver.}=7.3\%$, and standard deviation $|\Delta(J_c^d)|_{st.dev.}=6.9\%$. Results are even better for the relative difference and standard deviation in crack initiation time: $\Delta(t_i)_{aver.}=3.6\%$, $\Delta(t_i)_{st.dev.}=6.5\%$. Indeed, both techniques were successful in evaluating crack initiation, although some major difficulties in performing the tests were:

- stability of the specimen, because of the massive PD-input wire connections;
- selection of the optimal PD-input electric current and voltage, because it affects the output signal quality;
- specimen insulation from direct contact of the anvil and tup, in order to reduce amplitude noise probably developing from the power source and eddy currents;
- special attention should be made to the quality of the acquisition device, since the adequate selection of the coupling impedance of the input signal and proper grounding on all electric devices decreases noise.

The curves in Figs. 4 and 5 show J-integral vs. loading rate, and J-integral vs. initial crack length, respectively.

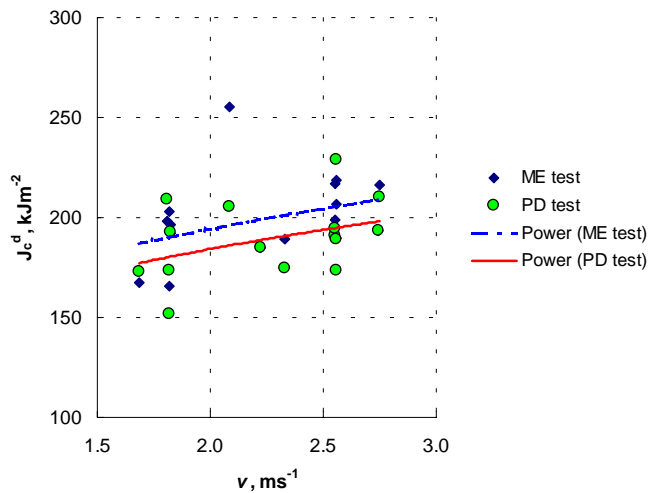


Figure 4. J_c^d – v dependence for MF and PD tests

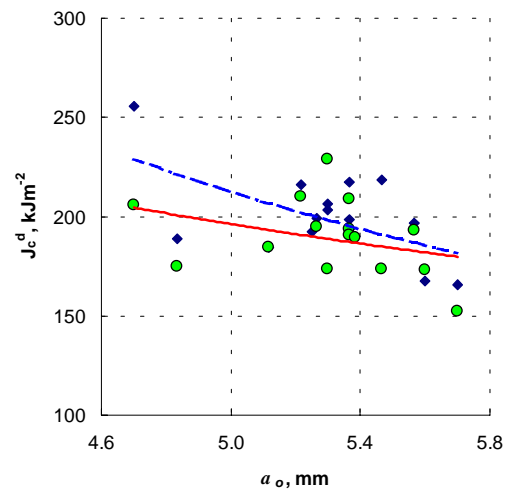


Figure 5. J_c^d – a_o dependence for MF and PD tests

CONCLUSIONS

Results shown in Figs. 4 and 5 have been statistically interpreted by power curves, although the result is the same if fitted by a linear, exponential, or logarithmic curve. This indicates an increasing tendency of the dynamic J-integral (J_c^d) with impact load rate (v), and a decreasing tendency for larger initial cracks (a_o). Fitted power curves $J=f(v^x)$, $J=f(a_o^x)$, show very small difference in J-integral, indicating good agreement between ME and PD techniques on evaluation of ductile crack growth initiation.

The ME power curve is constantly located above the PD power curve indicating slightly higher J-integral. In the average this is true, since PD evaluated time-to-fracture (t_i) is usually shorter than its ME equivalent (Table 2). So, the released energies $U(t)$ are smaller, and dynamic J-integral values are smaller too, Eq. (1). Multiple peaks in $F(t)$ -ME(t) and $F(t)$ -PD(t) diagrams are probably related to complex development of crack initiation and propagation. Analyses indicate that ME peaks follow PD peaks by a small delay, and both peaks usually precede $F(t)$ peaks. This is still not clear, but the delay is probably related to specimen–strain gauge, or specimen–probe interaction, or hysteresis in electric and magnetic properties of the tested material.

ACKNOWLEDGEMENTS

The authors gratefully acknowledge the support of the OTKA T 030057 project.

REFERENCES

1. Winkler, S.R. (1990). ASTM STP 1074, Philadelphia, pp.178-192.
2. Lenkey, Gy.B. (1997). In: 7th Summer School of Frac. Mech., Velika Plana, Yugoslavia, pp.39-50
3. Lenkey, Gy.B. and Winkler, S.R. (1997) *Fatigue and Fract. of Engng. Mater. and Struct.* 20, 143.
4. Lenkey, Gy.B. and Tóth, L. (2000). In: *Fracture Mechanics: Applications and Challenges*, Fuentes, M., Elices, M., Martin-Meizoso, A., and Martínez-Esnaola, J.M. (Eds.), Elsevier, Oxford.
5. Radakovic, Z., Lenkey, Gy.B. and Sedmak, A. (1998). In *Fracture from Defects*, Vol.III, pp.1267-1272, Brown, M.W., Rios, E.R. and Miller, K.J. (Eds.)
6. Glover, A.P., Johnson, F.A., Radon, J.C. and Turner, C.E. (1977). In: *ASM Int. Conf. on Dynamic Frac. Tough.*, Vol. 1, pp.63-75, The Welding Institute.
7. MacGillivray, H.J. and Turner, C.E. (1989). In: *Fourth Int. Conf. on the Mech. Properties of Mater. at High Rates of Strain*, Oxford.
8. Grabulov, V., MacGillivray, H.J., Tomic, D. and Jovanic, P. (1992). In: *Reliab. and struct. integ. of adv. materials*, pp.315-320, Sedmak, S., Sedmak, A. and Ruzic, D. (Eds.), EMAS, Warley West Midlands.
9. Grabulov, V. (1995). PhD Thesis, University of Belgrade, Depart. of Tech. and Metallurgy, Yugoslavia.
10. Radakovic, Z., Lenkey, Gy.B., Grabulov, V. and Sedmak, A. (1999) *Internat. Jour. of Frac.* 96, L23.
11. Yoon, J.H., Lee, B.S., Oh, Y.J. and Hong, J.H. (1999). *Inter. Jour. of Pres. Vessels and Piping* 76, 663.